

Nonclassical phonon pair

Yu Wang^{1,2,3#}, Zhen Shen^{1,2,3#}, Mai Zhang^{1,2,3#}, Zhi-Peng Shi^{1,2,3#}, Hong-Yi Kuang^{1,2,3},
Shuai Wan^{1,2,3}, Fang-Wen Sun^{1,2,3}, Guang-Can Guo^{1,2,3}, and Chun-Hua Dong^{1,2,3,*}

¹CAS Key Laboratory of Quantum Information, University of Science and Technology of China, Hefei, Anhui 230026, China

²CAS Center For Excellence in Quantum Information and Quantum Physics,

University of Science and Technology of China, Hefei, Anhui 230088, China and

³Hefei National Laboratory, University of Science and Technology of China, Hefei, Anhui 230088, China*

(Dated: October 1, 2025)

Quantum-correlated photon pairs are crucial resources for modern quantum information science. Similarly, the reliable generation of nonclassical phonon pairs is vital for advancing engineerable solid-state quantum devices and hybrid quantum networks based on phonons. Here, we present a novel approach to generate quantum-correlated phonon pairs in a suspended silicon microstructure initialized in its motional ground state. By simultaneously implementing red- and blue-detuned laser pulses, equivalent high-order optomechanical nonlinearity—specifically, an effective optomechanical four-wave mixing process—is achieved for generating a nonclassical phonon pair, which is then read out via a subsequent red-detuned pulse. We demonstrate the nonclassical nature of the generated phonon pair through the violation of the Cauchy–Schwarz inequality. Our experimentally observed phonon pair violates the classical bound by more than 5 standard deviations and maintains a decoherence time of 132 ns. This work reveals novel quantum manipulation of phonon states enabled by equivalent high-order optomechanical nonlinearity within a pulse scheme and provides a valuable quantum resource for mechanical quantum computing.

Introduction. - Quantum-correlated pairs are crucial resources for modern quantum information science and underpin a broad range of fundamental physical effects, including in distributed quantum computation, quantum communication, and quantum metrology [1–5]. Over the past decade, nonclassical particle pairs, particularly entangled photon pairs, have played a pivotal role in demonstrating the triumph of quantum physics over local realism through Bell inequality violations and are key components in modern quantum information protocols such as quantum repeaters, quantum memories, and device-independent quantum key distribution [6–10]. Entangled pairs have been demonstrated not only between various encoding photons [11–13] but also between photons and matter qubits, such as atoms [14], spins [15], phonons [16], and electrons [17]. These unique quantum resources are paramount for harnessing quantum correlations in hybrid quantum networks [18, 19].

Phonons, which are strikingly similar to photons, are emerging as promising candidates for engineerable solid-state quantum devices and quantum communication interfaces because of their ability to coherently interact with various quantum systems [16, 19–22]. This has spurred significant interest in quantum manipulation of phonon states, offering a novel platform in quantum information science. Advances in opto- and electromechanical domains include ground-state cooling [23], Fock state phonon manipulation [16, 24], entanglement of mechanical oscillators [25, 26], and quantum transducers [13]. In particular, significant recent advancements in surface acoustic wave platforms driven by strongly coupled su-

perconducting circuits have enabled impressive demonstrations of nonclassical phonon states, including multiphonon Fock states [24], phononic beam splitters [27], and mechanical qubits [28]. For typical optomechanical devices, which are key components of mechanical quantum elements, strong confinement of phonons leads to a longer lifetime and relatively small footprints, making them well suited for scaling to more complex circuits and performing multistage manipulation [29]. However, the generation of nonclassical phonon pairs via optical control remains challenging because of the limited strength of single photon optomechanical coupling and the underdeveloped exploitation of equivalent high-order optomechanical nonlinearity [28, 30, 31].

Here, we present a method for generating quantum-correlated phonon pairs from an optomechanical crystal (OMC) nanobeam cavity by leveraging effective high-order optomechanical nonlinearity, in which Stokes and anti-Stokes interactions are simultaneously implemented in one pulse. Analogous to the spontaneous parametric down-conversion (SPDC) process, the effective optomechanical spontaneous four-wave mixing (SFWM) process in our protocol creates a degenerate correlated phonon pair. The generated quantum correlated phonon pair is then retrieved by a second red-detuned pulse and verified by the well-known Cauchy–Schwarz inequality, which is a standard criterion for distinguishing classical from quantum correlations. Here we demonstrate not only that engineering the equivalent high-order optomechanical nonlinearity under a pulse scheme is possible but also that our protocol for quantum manipulation of phonon states could generate quantum resources for mechanical quantum computing.

Schematic of the nonclassical phonon pair generation. - Our protocol for generating quantum-

*Electronic address: chunhua@ustc.edu.cn

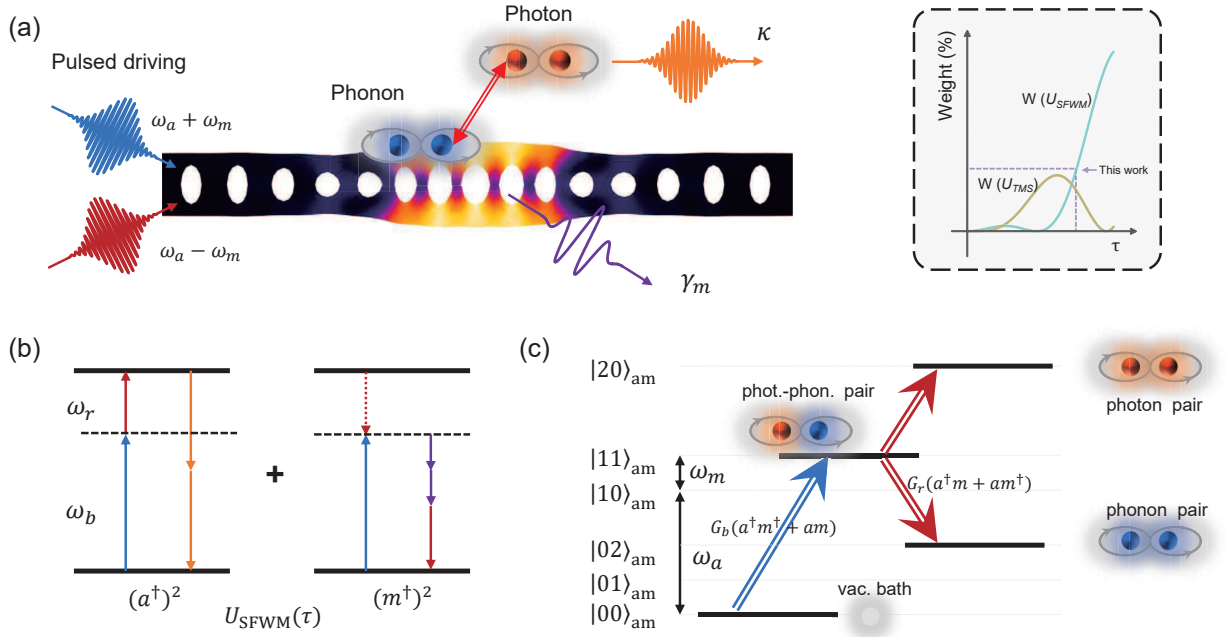


FIG. 1: **Schematic of the nonclassical phonon pair generation.** (a) An OMC nanobeam cavity is simultaneously driven by optical pulses at laser frequencies of $\omega_a \pm \omega_m$ to generate a photon pair $|20\rangle_{a,m}$ or a phonon pair $|02\rangle_{a,m}$. The inset graphically illustrates the “weight engineering” of linear and quadratic terms in $U(t)$ with a^\dagger (or m^\dagger) by adjusting the pulse duration τ . (b) Energy level diagrams of optomechanical SFWM for optical (left) and mechanical (right) effective counterparts. The entire process corresponds to the equivalent high-order optomechanical nonlinearity interaction in Eq. 1. (c) Optomechanical energy diagram describing a virtual process in which a photon–phonon pair $|11\rangle_{a,m}$ is first generated by a blue-detuned pump and then transitions to $|20\rangle_{a,m}$ or $|02\rangle_{a,m}$ via an interaction with a red-detuned pump.

correlated phonon pairs is schematically illustrated in Fig. 1 (a). The optomechanical cavity is simultaneously driven by optical pulses at laser frequencies of $\omega_a \pm \omega_m$, where $\omega_{a(m)}$ is the optical (mechanical) resonance. Two different types of interactions on the basis of cavity-enhanced Stokes and anti-Stokes Raman scattering occur at the same time, corresponding to “two-mode squeezing” and “beam-splitter” interactions [20]. The time-evolution operator is derived as $U(t) = e^{-iH_{\text{int}}t/\hbar}$, where $H_{\text{int}}/\hbar = g_o (\alpha_r a^\dagger m + \alpha_b a^\dagger m^\dagger + H.C.)$. Here g_o is the single photon optomechanical coupling rate. $\alpha_{r(b)}$ and a (m) are the annihilation operators for the red (blue)-detuned pump and the optical (mechanical) mode, respectively. The general linear term $U_{\text{TMS}}(t)$ in $U(t)$ describes “two-mode squeezing” on the basis of cavity-enhanced Stokes scattering [20]. Unusually, the quadratic term in $U(t)$,

$$U_{\text{SFWM}}(t) = c(t) \left[\alpha_r \alpha_b (a^\dagger)^2 m m^\dagger + \alpha_r^\dagger \alpha_b a a^\dagger (m^\dagger)^2 \right] + H.C. \quad (1)$$

represents an equivalent optomechanical SFWM process, where $c(t)$ is a time-dependent coefficient (see the Supplementary Information). The whole energy diagram for this process, shown in Fig. 1(b), is separated into optical and mechanical counterparts. The optical counterpart derived from the first term in Eq. (1), is analogous to the optical $\chi^{(3)}$ SFWM process [32]. The mechani-

cal counterpart derived from the second term in Eq. (1) describes the generation of an entangled phonon pair at ω_m via absorption of a pump photon α_b and release of a pump photon α_r . This can be equivalent to mechanical SPDC [11], in which an entangled phonon pair at ω_m is generated by the annihilation of a mechanical pump quantum at $2\omega_m$.

Therefore, when these optical pulses of duration τ are applied to the initial optomechanical vacuum state $|00\rangle_{a,m}$, the system evolves from the initial vacuum state to $|\varphi\rangle_{a,m} = U(\tau) |00\rangle_{a,m}$. The resulting optomechanical state is $|00\rangle_{a,m} + \sqrt{p_b(1-p_r)} |11\rangle_{a,m} + \sqrt{p_b p_r} |\Phi\rangle_{a,m} + O(p_b)$, where

$$|\Phi\rangle_{a,m} = \frac{1}{\sqrt{2}} (|20\rangle_{a,m} + |02\rangle_{a,m}) \quad (2)$$

is an optomechanical *NOON* state [33], and $p_r = \sin^2(2G_r\tau)$ and $p_b = G_b^2\tau^2$ represent the mean absorption probabilities of intracavity photons $n_{r(b)}$, with $G_{r(b)} = g_o \sqrt{n_{r(b)}}$. The evolution of $U_{\text{SFWM}}(t)$ can be intuitively described as a process in which a photon–phonon pair is first generated by absorption of a blue-detuned pump photon and subsequently transitions to either photon pair $|20\rangle_{a,m}$ or phonon pair $|02\rangle_{a,m}$ via absorption or release of a red-detuned pump photon, as shown in Fig. 1(c). Specifically, when $p_r = 1$, a purer optomechan-

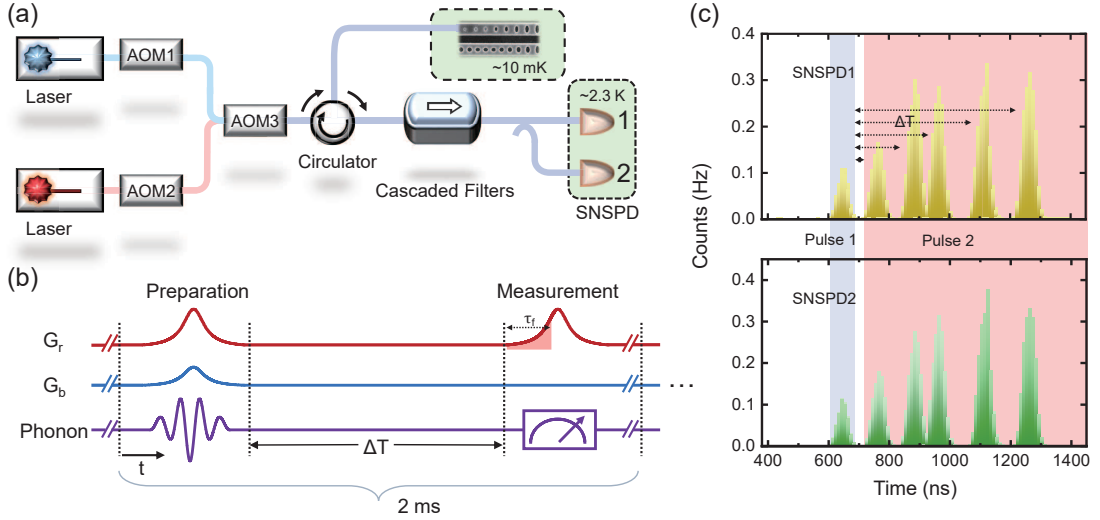


FIG. 2: (a) Experimental set-up. AOM, acousto-optic modulator; SNSPD, superconducting nanowire single-photon detector. (b) Schematic of the preparation-measurement protocol. The desired optomechanical quantum state $|\Phi\rangle_{a,m}$ is prepared via the first pulses and measured by the second red-detuned pulse which coherently retrieves phonons into signal photons and directly checks the nonclassical correlation of the phonon pair. The red shadow region with duration τ_f in the measurement pulse indicates the duration used for the statistics of twofold coincidence events. (c) Normalized counts of signal photons (ω_a) launched into two SNSPDs in the HBT setup during pulse 1 and pulse 2 for various preparation-measurement time delays ΔT . The purple and pink shadow areas represent the results for pulses 1 and 2, respectively.

ical *NOON* state $|\Phi\rangle_{a,m}$ can be created while the photon-phonon pair $|11\rangle_{a,m}$ is suppressed, which is inaccessible in the previous continuous driving quantum squeezing system [34]. Our pulse protocol allows engineering of the weights of different order terms in $U(t)$ by controlling G_r and τ , which promises the ability to highlight equivalent high-order optomechanical nonlinear effects, as depicted in the inset of Fig. 1(a). Notably, the resulting optomechanical states are distinct from the squeezing state and remain largely unexplored (see Supplementary Information). Limited by g_o and laser heating, our experimental demonstration is performed under $p_r < 1$, but this affects only the generation rates and purity of $|\Phi\rangle_{a,m}$.

Silicon optomechanical system. - The experimental setup is shown in Fig. 2(a). The OMC cavity, fabricated from a silicon-on-insulator (SOI) wafer [35, 36], exhibits an optical cavity resonance at wavelength $\lambda_a = 1550.589$ nm with a total damping rate $\kappa/2\pi \approx 700$ MHz and a mechanical “breathing” mode at a frequency of $\omega_m/2\pi \approx 5.2$ GHz with a damping rate of $\gamma_m/2\pi \approx 109$ kHz in a dilution refrigerator. The optical and mechanical modes are coupled via a combination of radiation pressure and photostriction with a single-photon optomechanical coupling rate of $g_o/2\pi = 800$ kHz, which is calibrated via sideband thermometry measurements [16]. In subsequent experiments, the pulse scheme, generated using acousto-optic modulators (AOMs) to avoid laser heating and optomechanical backaction, initializes the mechanical motion in its quantum ground state with a mean thermal phonon occupation $n_{th} = 0.014 \pm 0.004$ (see the Supplementary Information).

A preparation-measurement scheme, repeated every

2 ms, is implemented, as shown in Fig. 2(b). First, we prepare the desired optomechanical quantum state $|\Phi\rangle_{a,m}$ by applying the above unitary operator of Eq. 1. Owing to the short photon lifetime, the photon pair $|20\rangle_{a,m}$ generated with a probability of 1/2 is rapidly emitted from the cavity, whereas the phonon pair $|02\rangle_{a,m}$ also created with a probability of 1/2 persists for a moment. The preparation pulses with a full width at half maximum (FWHM) of 36 ns create $|\Phi\rangle_{a,m}$ with a probability of $p_{pre} = p_b p_r \approx 2.9\%$ (see the Supplementary Information). Consequently, the signal photons in pulse 1 contain the desired photon pair $|20\rangle_{a,m}$ and the inevitable scattered photons from the Stokes and anti-Stokes processes. The mechanical state is subsequently read out using a 47 ns (FWHM) red-detuned measurement pulse at various preparation-measurement time delays, ΔT , which indicate the interval between the end of the first pulse and the start of the second pulse and satisfy $1/\gamma_m > \Delta T \gg 1/\kappa$. The signal photons in pulse 2 contain photons coherently converted from the expected phonon pair $|02\rangle_{a,m}$ and unavoidable anti-Stokes scattering. The phonon-photon conversion probability p_{meas} is approximately 24.4%. The poor preparation probability is primarily limited by laser heating. The resulting signal photons (ω_a) are filtered by cascaded filters and launched into two superconducting nanowire single-photon detectors (SNSPDs) in a Hanbury Brown–Twiss (HBT) setup, as shown in Fig. 2(a). Figure 2(c) shows the normalized counts for the first and second pulses. These results are further used for twofold coincidence to verify nonclassical correlations. The increased counts in pulse 2 at longer ΔT are attributed to mechanical thermal relaxation (dis-

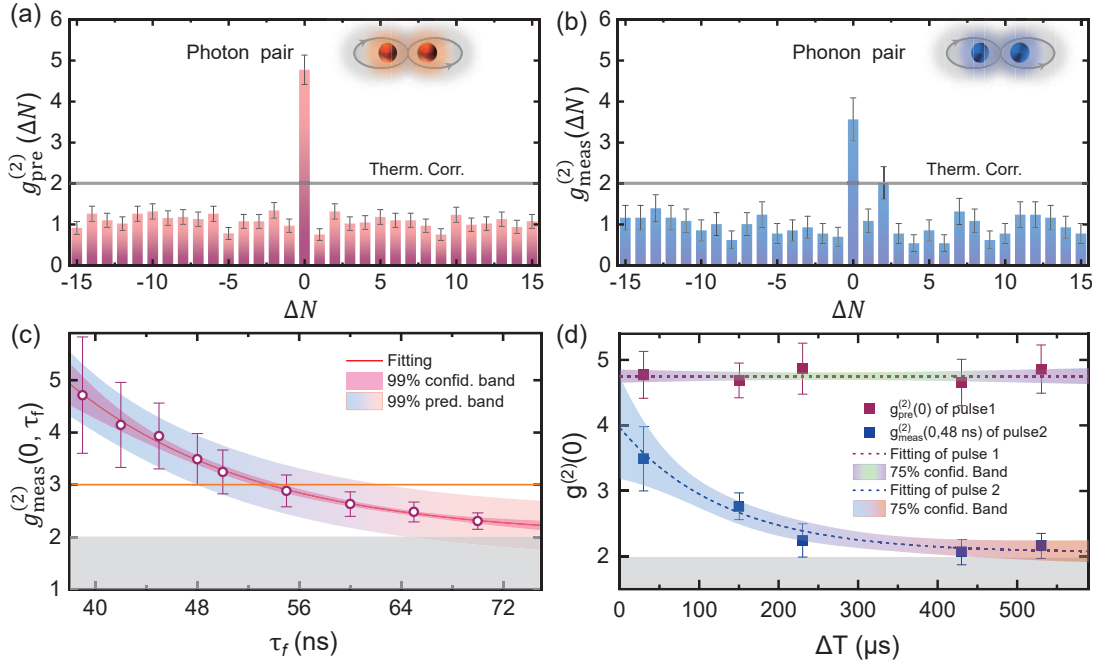


FIG. 3: **Experimental demonstration of a phonon pair.** (a-b) Experimental $g_{\text{pre}}^{(2)}(\Delta N)$ and $g_{\text{meas}}^{(2)}(\Delta N)$ for the preparation and measurement pulses, respectively. (c) Exponential decay $g_{\text{meas}}^{(2)}(0, \tau_f)$ as a function of τ_f with $\Delta T = 30$ ns. The red fitting line shows an exponential decay constant of $t_{d1} \approx 15$ ns. The shadow areas indicate the 99% confidence and prediction intervals. (d) shows almost identical $g_{\text{pre}}^{(2)}(0)$ values while $g_{\text{meas}}^{(2)}(0, 48 \text{ ns})$ decays into the thermal state as the time interval ΔT increases. The dashed blue line shows the fitted decoherence lifetime t_{d2} of approximately 132 ns. The shadow area indicates the 75% confidence interval. All error bars indicate \pm one standard deviation.

cussed later).

Experimental demonstration of a phonon pair.

-To confirm the generation of nonclassical phonon pairs, we employ the well-known Cauchy-Schwarz inequality [37]. Two phonons in $|02\rangle_{a,m}$ arise from two correlated pathways, i.e., $|02\rangle_{a,m} = |0\rangle_a |1_b 1_r\rangle_m$: (I) directly from a single Stokes scattering event, and (II) through conversion from a previously generated photon via anti-Stokes scattering. The noncanonical correlations between them are quantified by deriving a modified Cauchy-Schwarz inequality. For the second-order correlation function $g^{(2)}$ of signal photons in this process, we obtain,

$$g^{(2)} \leq \frac{\eta^2 g_r^{(2)} + g_b^{(2)} + 4\eta \sqrt{g_r^{(2)} g_b^{(2)}}}{(1 + \eta)^2}, \quad (3)$$

where $g_{r(b)}^{(2)}$ is the second-order correlation of the scattering photons driven solely by the red (blue)-detuned laser and η is related to the ratio of the two Raman scattering rates. The right-hand side of inequality 3 is maximized when $\eta = 1$ for $g_r^{(2)} = g_b^{(2)}$ (see the Supplementary Information). Consequently, for a pair correlation of classical origin, a stricter boundary applies: $g^{(2)} \leq \frac{3}{2} \sqrt{g_r^{(2)} g_b^{(2)}}$. Therefore, the nonclassical nature of the phonon pair could be doubtlessly verified by violation of Eq. 3.

Figure 3(a) displays the second-order correlation func-

tion $g_{\text{pre}}^{(2)}(\Delta N)$ of signal photons for the preparation pulse, which is statistically obtained from numerous repeated pulse sequences of different trials separated by ΔN iterations. $g_{\text{pre}}^{(2)}(\Delta N)$ quantifies the quantum correlation of the generated photon pair in pulse 1, while the phonon pair is optionally created at the same rate. The typical values of $g_{\text{pre}}^{(2)}(\Delta N \neq 0)$ are close to 1, indicating that signal photons emerging from different pulse sequences are uncorrelated and that the Cauchy-Schwarz inequality is fulfilled. In contrast, for pairs emitted from the same pulse sequence ($\Delta N = 0$), $g_{\text{pre}}^{(2)}(0) = 4.8 \pm 0.4$, which significantly violates the classical bound by approximately 5 standard deviations, i.e.,

$$[g_{\text{pre}}^{(2)}(0)]^2 \not\leq 9 [g_{\text{pre,b}}^{(2)}(0) g_{\text{pre,r}}^{(2)}(0)] / 4,$$

where $g_{\text{pre,b}}^{(2)}(0) = 1.90 \pm 0.24$, and $g_{\text{pre,r}}^{(2)}(0) = 1.88 \pm 0.42$ (see the Supplementary Information). This violation of the Cauchy-Schwarz inequality unequivocally demonstrates the nonclassical correlation of photon pair $|20\rangle_{a,m}$.

For state $\Phi_{a,m}$, phonon pair $|02\rangle_{a,m}$ is produced in exactly the same way as optical state $|20\rangle_{a,m}$ and possesses the same quantum properties in principle. Direct mapping of mechanical state $|02\rangle_{a,m}$ via a second pulse, as shown in Fig. 3(b), would offer more intuitive evidence of entangled phonon pair generation. However, the $g_{\text{meas}}^{(2)}(0)$ for mechanical state $|02\rangle_{a,m}$ is worsened by

the initial n_{th} and additional heating from pulse 2, as shown in Fig. 3(c). Exponential decay fitting (red line) reveals a decay constant of $t_{\text{d1}} \approx 15$ ns, suggesting accelerated thermal decoherence due to the additional laser driving. The shorter the τ_f of pulse 2 is to mitigate laser heating from this pulse, the higher $g_{\text{meas}}^{(2)}(0)$ is. Notably, $g_{\text{meas}}^{(2)}(0, 39 \text{ ns}) = 4.7 \pm 1.1$, which is beyond the classical bound by approximately 1.5 standard deviations, although with larger error bars. Within the 99% prediction interval, the classical bound is undoubtedly violated for τ_f up to 48 ns. Therefore, we use click events during the first 48 ns of pulse 2 to maximize the coincidence counts of the entangled pair. The resulting $g_{\text{meas}}^{(2)}(\Delta N, 48 \text{ ns})$ is shown in Fig. 3(b). $g_{\text{meas}}^{(2)}(0, 48 \text{ ns}) = 3.5 \pm 0.5$ violates the Cauchy-Schwarz inequality,

$$\left[g_{\text{meas}}^{(2)}(0, 48 \text{ ns}) \right]^2 \not\leq 9 \left[g_{\text{meas},r}^{(2)}(0) \right]^2 / 4,$$

where $g_{\text{meas},r}^{(2)}(0) = 1.92 \pm 0.14$ (see the Supplementary Information), and deviates from the thermal state by 3.1 standard deviations. Additionally, Fig. 3(d) shows that $g_{\text{meas}}^{(2)}(0, 48 \text{ ns})$ decreases toward the thermal state as ΔT increases, whereas $g_{\text{pre}}^{(2)}(0)$ remains almost unchanged, where the shadow area indicates the 75% confidence interval. The fitted decoherence lifetime $t_{\text{d2}} = 132$ ns demonstrates that we can store and retrieve the non-classical mechanical state $|02\rangle_{\text{a,m}}$ for an extended time interval.

To rule out the possibility of direct excitation of state $|22\rangle_{\text{a,m}}$ by the blue-detuned drive, we analyze fourfold coincidence counts of two-photon click events n_{22} between pulses 1 and 2. Figure 4(a) shows the results for $N \approx 1.4 \times 10^8$ independent equally distributed experiments with $\Delta T = 150$ ns. We observe $n_{22} = 0$, whereas the coincidence counts between two-photon click events in pulse 1 (2) and zero-photon click events in pulse 2 (1) are significantly greater. This result indicates negligible excitation of state $|22\rangle_{\text{a,m}}$. Moreover, the pair events generated in the two pulses exhibit mutual repulsion, which is consistent with the behavior of the declared state $|\Phi\rangle_{\text{a,m}} = (|20\rangle_{\text{a,m}} + |02\rangle_{\text{a,m}}) / \sqrt{2}$. Consequently, the use of pair events $|20\rangle_{\text{a,m}}$ in pulse 1 allows post-selection of a mechanical vacuum state. Conversely, the detection of zero-photon events $|00\rangle_{\text{a,m}}$ in pulse 1 projects state $|\varphi\rangle_{\text{a,m}}$ to

$$|\varphi'\rangle_{\text{a,m}} = |00\rangle_{\text{a,m}} + \sqrt{p_{\text{b}}/p_{\text{r}}} |02\rangle_{\text{a,m}} + O(p_{\text{b}}), \quad (4)$$

effectively doubling the phonon pair probability. In this scenario, the generation rate of the phonon pair is $\propto p_{\text{b}}$, surpassing the p_{b}^2 rate achievable with only “two-mode squeezed” interaction.

To identify the limitations on the storage time of the phonon pair, we measure the mechanical mode decay lifetime using a pump-probe scheme, as shown in Fig. 4(b). A short blue-detuned pulse (pump) excites phonon

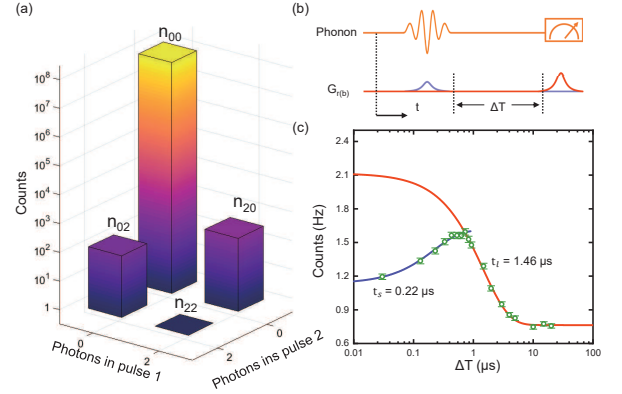


FIG. 4: (a) Coincidence counts of two-photon click events and zero-photon click events between pulses 1 and 2, obtained from $N \approx 1.4 \times 10^8$ independent equally distributed experiments with $\Delta T = 150$ ns. (b) Pump-probe measurement in mechanical breathing mode. A short blue-detuned pulse (pump) is sent to excite phonon occupation, and then, the mechanical response is measured via a red-detuned optical probe pulse as a function of the pump-probe time delay ΔT . (c) The red and blue lines are the exponential theoretical fits, corresponding to $t_l = 1.46 \mu\text{s}$ and $t_s = 0.22 \mu\text{s}$, respectively. All error bars indicate \pm one standard deviation.

occupation, and then the mechanical response is measured by a red-detuned probe pulse as a function of the pump-probe time delay (ΔT). Figure 4(c) displays the results. The long-term mechanical response ($\Delta T \geq 1 \mu\text{s}$) well fits a simple exponential decay (red line) with a decay time constant (t_l) of $1.46 \mu\text{s}$, which is consistent with the mechanical Q_{m} of 4.8×10^4 . However, the short-term mechanical response ($\Delta T < 1 \mu\text{s}$) shows mechanical thermal relaxation due to laser heating. The mechanical thermal relaxation time can be fitted to another exponential curve with a time constant of $t_s = 0.22 \mu\text{s}$ (blue line). The scale of t_s is consistent with t_{d2} and with the increasing count rates in Fig. 2(c). Therefore, the quantum properties of our phonon pair are limited primarily by laser-induced mechanical thermal relaxation, which drives the mechanical system toward the thermal state.

Unlike previous work on quantum squeezing [34] and quantum nondemolition measurement [38] of continuous variables (typically employing homodyne or heterodyne detection of two tones of a continuous pump), our experiment utilizes a pulse scheme. This approach enables access to the evolution of discrete quantum variables using the equivalent high-order optomechanical nonlinearity, offering the potential to control the evolutionary phases of individual states through the driving intensity and duration. Here, we have generated quantum-correlated phonon pairs via optical control based on the quadratic term in the time-evolution operator $U(t)$. The dominant limitation originates from the heating induced by both the preparation and measurement pulses, and even better results can be expected by further reducing the laser heating, such as when 2D OMC structures are used [39].

Conclusion. - In summary, this work demonstrates, for the first time, the generation and verification of quantum correlated phonon pairs via optical control based on effective optomechanical SFWM and violation of the Cauchy–Schwarz inequality. A pulse scheme enables access to equivalent high-order optomechanical nonlinearity—primarily an effective optomechanical SFWM process here—facilitating the creation of an optomechanical NOON state and the conditional generation of

a quantum-correlated phonon pair. Our experiments demonstrate violations of the Cauchy–Schwarz inequality by over 5 standard deviations for the photon pair and 1.5 standard deviations for the phonon pair. The decoherence lifetime of the phonon pair is 132 ns. This research opens new avenues for experimentally exploring effective high-order nonlinearity in quantum optomechanics, and expands the available techniques for quantum optomechanical manipulation.

-
- [1] H. J. Kimble, “The quantum internet,” *Nature* **453**, 1023 (2008).
 - [2] P. Walther, K. J. Resch, T. Rudolph, E. Schenck, H. Weinfurter, V. Vedral, M. Aspelmeyer, and A. Zeilinger, “Experimental one-way quantum computing,” *Nature* **434**, 169 (2005).
 - [3] V. Giovannetti, S. Lloyd, and L. Maccone, “Quantum-enhanced measurements: beating the standard quantum limit,” *Science* **306**, 1330 (2004).
 - [4] J. L. O’Brien, A. Furusawa, and J. Vučković, “Photonic quantum technologies,” *Nature Photonics* **3**, 687 (2009).
 - [5] L. Pezze, A. Smerzi, M. K. Oberthaler, R. Schmied, and P. Treutlein, “Quantum metrology with nonclassical states of atomic ensembles,” *Reviews of Modern Physics* **90**, 035005 (2018).
 - [6] M. Giustina, M. A. Versteegh, S. Wengerowsky, J. Handsteiner, A. Hochrainer, K. Phelan, F. Steinlechner, J. Kofler, J.-Å. Larsson, C. Abellán, *et al.*, “Significant-loophole-free test of Bell’s theorem with entangled photons,” *Physical review letters* **115**, 250401 (2015).
 - [7] N. Sangouard, C. Simon, H. De Riedmatten, and N. Gisin, “Quantum repeaters based on atomic ensembles and linear optics,” *Reviews of Modern Physics* **83**, 33 (2011).
 - [8] X. Liu, J. Hu, Z.-F. Li, X. Li, P.-Y. Li, P.-J. Liang, Z.-Q. Zhou, C.-F. Li, and G.-C. Guo, “Heralded entanglement distribution between two absorptive quantum memories,” *Nature* **594**, 41 (2021).
 - [9] A. Wallucks, I. Marinković, B. Hensen, R. Stockill, and S. Gröblacher, “A quantum memory at telecom wavelengths,” *Nature Physics* **16**, 772 (2020).
 - [10] A. Acín, N. Brunner, N. Gisin, S. Massar, S. Pironio, and V. Scarani, “Device-independent security of quantum cryptography against collective attacks,” *Physical Review Letters* **98**, 230501 (2007).
 - [11] J.-W. Pan, Z.-B. Chen, C.-Y. Lu, H. Weinfurter, A. Zeilinger, and M. Żukowski, “Multiphoton entanglement and interferometry,” *Reviews of Modern Physics* **84**, 777 (2012).
 - [12] A. S. Sheremet, M. I. Petrov, I. V. Iorsh, A. V. Poshakinskiy, and A. N. Poddubny, “Waveguide quantum electrodynamics: Collective radiance and photon-photon correlations,” *Reviews of Modern Physics* **95**, 015002 (2023).
 - [13] S. Meesala, S. Wood, D. Lake, P. Chiappina, C. Zhong, A. D. Beyer, M. D. Shaw, L. Jiang, and O. Painter, “Non-classical microwave–optical photon pair generation with a chip-scale transducer,” *Nature Physics* , 1 (2024).
 - [14] J. Volz, M. Weber, D. Schlenk, W. Rosenfeld, J. Vrana, K. Saucke, C. Kurtsiefer, and H. Weinfurter, “Observation of entanglement of a single photon with a trapped atom,” *Physical review letters* **96**, 030404 (2006).
 - [15] W. Gao, P. Fallahi, E. Togan, J. Miguel-Sánchez, and A. Imamoglu, “Observation of entanglement between a quantum dot spin and a single photon,” *Nature* **491**, 426 (2012).
 - [16] R. Riedinger, S. Hong, R. A. Norte, J. A. Slater, J. Shang, A. G. Krause, V. Anant, M. Aspelmeyer, and S. Gröblacher, “Non-classical correlations between single photons and phonons from a mechanical oscillator,” *Nature* **530**, 313 (2016).
 - [17] A. Feist, G. Huang, G. Arend, Y. Yang, J.-W. Henke, A. S. Raja, F. J. Kappert, R. N. Wang, H. Lourenço-Martins, Z. Qiu, *et al.*, “Cavity-mediated electron-photon pairs,” *Science* **377**, 777 (2022).
 - [18] A. Clerk, K. Lehnert, P. Bertet, J. Petta, and Y. Nakamura, “Hybrid quantum systems with circuit quantum electrodynamics,” *Nature Physics* **16**, 257 (2020).
 - [19] Z. Shen, G.-T. Xu, M. Zhang, Y.-L. Zhang, Y. Wang, C.-Z. Chai, C.-L. Zou, G.-C. Guo, and C.-H. Dong, “Coherent coupling between phonons, magnons, and photons,” *Physical Review Letters* **129**, 243601 (2022).
 - [20] M. Aspelmeyer, T. J. Kippenberg, and F. Marquardt, “Cavity optomechanics,” *Reviews of Modern Physics* **86**, 1391 (2014).
 - [21] C. Dong, V. Fiore, M. C. Kuzyk, and H. Wang, “Optomechanical dark mode,” *Science* **338**, 1609 (2012).
 - [22] Y. Wang, M. Zhang, Z. Shen, G.-T. Xu, R. Niu, F.-W. Sun, G.-C. Guo, and C.-H. Dong, “Optomechanical frequency comb based on multiple nonlinear dynamics,” *Physical Review Letters* **132**, 163603 (2024).
 - [23] J. Chan, T. M. Alegre, A. H. Safavi-Naeini, J. T. Hill, A. Krause, S. Gröblacher, M. Aspelmeyer, and O. Painter, “Laser cooling of a nanomechanical oscillator into its quantum ground state,” *Nature* **478**, 89 (2011).
 - [24] Y. Chu, P. Kharel, T. Yoon, L. Frunzio, P. T. Rakich, and R. J. Schoelkopf, “Creation and control of multiphonon fock states in a bulk acoustic-wave resonator,” *Nature* **563**, 666 (2018).
 - [25] R. Riedinger, A. Wallucks, I. Marinković, C. Löschner, M. Aspelmeyer, S. Hong, and S. Gröblacher, “Remote quantum entanglement between two micromechanical oscillators,” *Nature* **556**, 473 (2018).
 - [26] E. A. Wollack, A. Y. Cleland, R. G. Gruenke, Z. Wang, P. Arrangoiz-Arriola, and A. H. Safavi-Naeini, “Quantum state preparation and tomography of entangled mechanical resonators,” *Nature* **604**, 463 (2022).
 - [27] H. Qiao, É. Dumur, G. Andersson, H. Yan, M.-H. Chou, J. Grebel, C. Conner, Y. Joshi, J. Miller, R. Povey, *et al.*, “Splitting phonons: Building a platform for linear mechanical quantum computing,” *Science* **380**, 1030 (2023).

- [28] Y. Yang, I. Kladarić, M. Drimmer, U. von Lüpke, D. Lentnerman, J. Bus, S. Marti, M. Fadel, and Y. Chu, “A mechanical qubit,” *Science* **386**, 783 (2024).
- [29] A. Zivari, N. Fiaschi, L. Scarpelli, M. Jansen, R. Burgwal, E. Verhagen, and S. Gröblacher, “A single-phonon directional coupler,” arXiv preprint arXiv:2312.04414 (2023).
- [30] P. Arrangoiz-Arriola, E. A. Wollack, Z. Wang, M. Pechal, W. Jiang, T. P. McKenna, J. D. Witmer, R. Van Laer, and A. H. Safavi-Naeini, “Resolving the energy levels of a nanomechanical oscillator,” *Nature* **571**, 537 (2019).
- [31] T. Kuang, R. Huang, W. Xiong, Y. Zuo, X. Han, F. Nori, C.-W. Qiu, H. Luo, H. Jing, and G. Xiao, “Nonlinear multi-frequency phonon lasers with active levitated optomechanics,” *Nature Physics* **19**, 414 (2023).
- [32] J. W. Silverstone, D. Bonneau, K. Ohira, N. Suzuki, H. Yoshida, N. Iizuka, M. Ezaki, C. M. Natarajan, M. G. Tanner, R. H. Hadfield, *et al.*, “On-chip quantum interference between silicon photon-pair sources,” *Nature Photonics* **8**, 104 (2014).
- [33] I. Afek, O. Ambar, and Y. Silberberg, “High-noon states by mixing quantum and classical light,” *Science* **328**, 879 (2010).
- [34] E. E. Wollman, C. Lei, A. Weinstein, J. Suh, A. Kronwald, F. Marquardt, A. A. Clerk, and K. Schwab, “Quantum squeezing of motion in a mechanical resonator,” *Science* **349**, 952 (2015).
- [35] J. Chan, A. H. Safavi-Naeini, J. T. Hill, S. Meenehan, and O. Painter, “Optimized optomechanical crystal cavity with acoustic radiation shield,” *Applied Physics Letters* **101** (2012).
- [36] Y. Wang, Z.-P. Shi, H.-Y. Kuang, X. Xi, S. Wan, Z. Shen, P.-Y. Wang, G.-T. Xu, X. Sun, C.-L. Zou, *et al.*, “Realization of quantum ground state in an optomechanical crystal cavity,” *Science China Physics, Mechanics & Astronomy* **66**, 124213 (2023).
- [37] A. Kuzmich, W. Bowen, A. Boozer, A. Boca, C. Chou, L.-M. Duan, and H. Kimble, “Generation of nonclassical photon pairs for scalable quantum communication with atomic ensembles,” *Nature* **423**, 731 (2003).
- [38] C. Lei, A. Weinstein, J. Suh, E. Wollman, A. Kronwald, F. Marquardt, A. Clerk, and K. Schwab, “Quantum non-demolition measurement of a quantum squeezed state beyond the 3 db limit,” *Physical review letters* **117**, 100801 (2016).
- [39] L. Chen, A. R. Korsch, C. M. Kersul, R. Benevides, Y. Yu, T. P. M. Alegre, and S. Gröblacher, “Bandwidth-tunable telecom single photons enabled by low-noise optomechanical transduction,” arXiv preprint arXiv:2410.10947 (2024).

Acknowledgments.-The authors would like to thank H. Wang and Y. Guo for discussions. This work was supported by the Innovation program for Quantum Science and Technology (2021ZD0303203), National Natural Science Foundation of China (Grant No.12293052, 12293050, 11934012, 12474394, 12104442, 12447139 and 92250302), the China Postdoctoral Science Foundation (Grant No. 2024T008AH), the Natural Science Foundation of Anhui Province (Grant No. 2308085J12 and 2408085QA021), the Fundamental Research Funds for the Central Universities, USTC Major Frontier Research Program (LS2030000002), and the CAS Project for Young Scientists in Basic Research (YSBR-069). This work was partially carried out at the USTC Center for Micro and Nanoscale Research and Fabrication.

Author contributions.-Y.W., Z.S. and C.H.D. conceived the experiment. Y.W., H.Y.K., and S.W. performed the device design and fabrication. Y.W., Z.S., Z.P.S. and C.H.D. performed the measurements, analyzed the data. M.Z. and Y.W. performed the theoretical simulation and classical-quantum criterion derivation, F.W.S. provided theoretical support. Y.W., Z.S., M.Z. and C.H.D. wrote the manuscript. C.H.D. and G.C.G. supervised the project.

Competing interests.-The authors declare no competing interests.

Additional information.-Supplementary information is available online. Correspondence and requests for materials should be addressed to C.-H.D.